Galvanomagnetic Effects in Oriented Single Crystals of *n*-Type Germanium*

W. MURRAY BULLIS†
Lincoln Laboratory and Department of Physics, Massachusetts Institute of Technology, Cambridge, Massachusetts
(Received August 5, 1957)

Measurements of the magnetoresistance, Hall, and planar Hall coefficients have been made on oriented single crystals of *n*-type germanium at 77° and 300°K. At 77°K measurements made as a function of the magnetic field strength and of the angle between the current and the magnetic field are found to be in agreement with theoretical calculations based on an energy-independent mean free time τ_0 which has the same form of anisotropy as the effective mass at the bottom of the conduction band. The value of τ_0 is determined from previously described Hall measurements and the anisotropy factor K is determined from the high-field longitudinal magnetoresistance. K decreases from about 16 to about 12 or 13 as the electron density increases from about 5.4 $\times 10^{13}$ cm^{-3} to about 5.2$\times 10^{14}$ cm^{-3}.

At 300°K measurements were made for selected orientations of current and field on samples whose resistivities varied from 0.016 to 8.9 ohm-cm. The usual low-field symmetry relations are satisfied. Most of the low-field coefficients may be satisfactorily interpreted by means of relatively simple functional relationships between the mean free time τ and the energy $\mathcal{E}$. Although the field dependence of the Hall coefficient cannot be quantitatively explained in this manner, the qualitative features of the various Hall curves may be understood. Above 0.1 ohm-cm, K is found to be about 17.3 independent of the relationship between τ and $\mathcal{E}$. Below 0.1 ohm-cm, K falls off, reaching about 14 at 0.016 ohm-cm.

The decrease in the value of K as the temperature is lowered or as the impurity concentration is increased is attributed to an increase in the scattering anisotropy as impurity scattering becomes more important. With the assumption that the mass anisotropy is constant with temperature and impurity density, the magnitude of the scattering anisotropy can be computed.

I. INTRODUCTION

A PREVIOUS paper[1] has shown that calculations of the Hall coefficient using an energy-independent mean free time τ_0 and the 4- or 8-ellipsoid model[2–7] for the bottom of the conduction band, yield results which agree reasonably well with experimental values of the Hall voltage measured at 77°K in *n*-type germanium. It was shown that the proper value of τ_0 to be used in the calculations could be found from measurements of the Hall coefficient but that the value of the anisotropy factor K to be used could not be found from such measurements alone.

Other authors[8–12] have investigated the magnetoresistance effect in *n*-type germanium and interpreted their results on the basis of a low-field approximation[2,13] for the conductivity tensor. Mason, Hewitt, and Wick[14] investigated the Hall effect and interpreted their data in a similar fashion. In much of this work, lattice scattering was assumed to prevail and the mean free time was represented by a constant mean-free-path approximation, but some authors[10,11] employed more complicated expressions for the mean free time.

In the present work, measurements of the magnetoresistance, Hall, and planar Hall[8] coefficients made on a series of oriented single-crystal slabs of *n*-type germanium at 77° and 300°K will be described. The results of theoretical calculations will be summarized and compared with the data. Effective values of both K and τ_0 will be deduced from the 77°K data assuming an anisotropic but energy-independent mean free time. The 300°K data will be interpreted on the basis of the low-field approximation for the conductivity tensor and various simplifying approximations for the energy dependence of the mean free time τ.

TABLE I. Galvanomagnetic coefficients for current and magnetic field in specified directions calculated by using an energy-independent mean free time.

J	B	Coefficient	Expression[a]
(001)	[001]	M_t+1	$p/(1+z^2b^2)$
[001]	[001]	M_l+1	$p/(1+yb^2)$
[100]	[110]	$M_{100}+1$	$N_1'/D'F'$
[001]	[110]	$M_{001}+1$	$N_4'/D'F'$
[110]	[110]	$M_{110}+1$	$(N_1'+\frac{1}{2}N_3')/D'F'$
[1$\bar{1}$0]	[110]	$M_{1\bar{1}0}+1$	$(N_1'-\frac{1}{2}M_3')/D'F'$
[100]	[110]	$P_{100}B^2/\rho_0$	$N_3'/D'F'$
(001)	[001]	R^{001}/R_∞	$yKzp/(1+z^2b^2)$
[1$\bar{1}$0], [100], [001]	[110]	R^{110}/R_∞	$yKN_2'/D'F'$

[a] In these expressions $p=1+[(K+2)b^2/3K]$, $q=(2K+1)/3K^2$, $s=2(K-1)/3K$, $u=\frac{1}{2}xb^2$, $x=s(z-y)/p$, $y=3/(2K+1)$, $z=(K+2)/(2K+1)$, $N_1'=\frac{1}{2}[2+yb^2(z-u)^2]$, $N_3'=(1+yb^2+u)(z-u)$, $N_2'=b^2[(z-u)^2-(x+y)]$, $N_4'=1+yb^2-u(yb^2+u)$, $D'=(1+yb^2+u)[1-u(z-u)^2]$, $F'=p/(2p-1+qb^4)$, $b=\sigma_0R_0B/z=eB\tau_0/m_tc$, e=electronic charge (esu), c=velocity of light (cm/sec), $R_\infty=1/Nec$, N=number of electrons per cm^3, $m_t=0.082\ m_0$, and m_0=electron mass.

* This research was done at the Lincoln Laboratory of Massachusetts Institute of Technology which is jointly supported by the Army, Navy, and Air Force under contract with the Massachusetts Institute of Technology. This paper is based on a thesis submitted to the Department of Physics in partial fulfillment of the requirements for the degree of Doctor of Philosophy, June 1956. A preliminary account of some of this work was presented at the 1955 Thanksgiving Meeting of the American Physical Society.

† Now at Farnsworth Electronics Company, Fort Wayne, Indiana.

[1] W. M. Bullis and W. E. Krag, Phys. Rev. **101**, 580 (1956).
[2] B. Abeles and S. Meiboom, Phys. Rev. **95**, 31 (1954).
[3] M. Shibuya, Phys. Rev. **95**, 1385 (1954).
[4] L. Gold and L. M. Roth, Phys. Rev. **103**, 61 (1956).
[5] C. Herring, Bell System Tech. J. **34**, 237 (1955).
[6] C. Herring and E. Vogt, Phys. Rev. **101**, 944 (1956).
[7] Dexter, Zeiger, and Lax, Phys. Rev. **104**, 637 (1956).
[8] C. Goldberg and R. E. Davis, Phys. Rev. **94**, 1121 (1954).
[9] G. L. Pearson and H. Suhl, Phys. Rev. **83**, 768 (1951).
[10] Benedek, Paul, and Brooks, Phys. Rev. **100**, 1129 (1955).
[11] C. Goldberg and R. E. Davis, Phys. Rev. **102**, 1254 (1956).
[12] G. C. Della Pergola and D. Sette, Phys. Rev. **104**, 598 (1956).
[13] F. Seitz, Phys. Rev. **79**, 372 (1950).
[14] Mason, Hewitt, and Wick, J. Appl. Phys. **24**, 166 (1953).

TABLE II. Galvanomagnetic coefficients for the magnetic field restricted to the (001)-plane calculated by using an energy-independent mean free time.

J	$M+1$ [a]	R [a]	PB^2/ρ_0 [a]
[100]	$N_1(\alpha,\beta)/DF$	$yKR_\infty N_2(\alpha,\beta)/DF$	N_3/DF
[110]	$[N_1(\alpha,\beta)+N_1(\beta,\alpha)+2\alpha\beta N_3]/2DF$	$yKR_\infty[\beta N_2(\alpha,\beta)-\alpha N_2(\beta,\alpha)]/[DF(\beta-\alpha)]$	$[N_1(\beta,\alpha)-N_1(\alpha,\beta)]/[DF(\beta^2-\alpha^2)]$
[001]	N_4/DF	$yKR_\infty[\alpha^2 N_2(\beta,\alpha)+\beta^2 N_2(\alpha,\beta)]/DF$	none

[a] In these expressions $N_1(\alpha,\beta)=(1+yb^2\beta^2)+b^2\alpha^2(z-b^2\beta^2x)^2$, $N_2(\alpha,\beta)=b^2\alpha^2(x+y)(z-b^2\beta^2x)+(1+yb^2\beta^2)(z-b^2\alpha^2x)$, $N_3=b^2[(z-b^2\alpha^2x)(z-b^2\beta^2x)-(x+y)]$, $N_4=1+yb^2-b^4\alpha^2\beta^2x(x+2y)$, $D=\{(1+yb^2)(1+z^2b^2)-xb^4\alpha^2\beta^2[(x+2y)(1+2zb^2)-2z(z-2)-xb^2]+2x^2b^8\alpha^4\beta^4(x+2y)\}$, $F=p/(p^2-s^2b^4\alpha^2\beta^2)$, α = direction cosine of **B** with respect to the [100] axis and β = direction cosine of **B** with respect to the [010] axis.

II. THEORY AND CALCULATIONS

If **J** is the current density in a sample placed in a magnetic field **B**, the magnetoresistance coefficient M is given by

$$M+1=(\mathbf{E}\cdot\mathbf{J})/(\mathbf{E}\cdot\mathbf{J})_{B=0}, \tag{1}$$

the Hall coefficient R is given by

$$R=\mathbf{E}\cdot(\mathbf{J}\times\mathbf{B})/(\mathbf{J}\times\mathbf{B})^2, \tag{2}$$

and the planar Hall coefficient P is given by

$$P=[\mathbf{E}\cdot(\mathbf{J}\times\mathbf{B})\times\mathbf{J}]/(\mathbf{J}\times\mathbf{B})^2(\mathbf{J}\cdot\mathbf{B}), \tag{3}$$

where **E** is the total electric field in the crystal. It will be observed that these coefficients are respectively proportional to the component of **E** in the direction (1) of the current, (2) perpendicular to both the current and magnetic field, and (3) perpendicular to the current but in the plane of the current and magnetic field.

By substituting $\rho\mathbf{J}$ for **E** in Eqs. (1) to (3), the three galvanomagnetic coefficients may be expressed in terms of the resistivity tensor ρ. The elements of this tensor may be derived from the Boltzmann equation provided that suitable simplifying assumptions are made. This derivation has been carried out in considerable detail elsewhere[15] for a single-carrier model in homogeneous, isothermal material. It was assumed that Maxwell-Boltzmann statistics applied, that the surfaces of constant energy near the bottom of the conduction band could be represented by ellipsoids of revolution with the axis of revolution along the $\langle 111\rangle$ axes of the crystal, and that each energy minimum could be treated independently during the integration over momentum space. In the coordinate system of the principal axes of the ellipsoid of revolution, the mass tensor is diagonal:

$$m=\begin{bmatrix} m_t & 0 & 0 \\ 0 & m_t & 0 \\ 0 & 0 & m_l \end{bmatrix}. \tag{4}$$

In the same coordinate system, the mean free time is assumed to have the tensor form[6]

$$\tau=\begin{bmatrix} \alpha_t & 0 & 0 \\ 0 & \alpha_t & 0 \\ 0 & 0 & \alpha_l \end{bmatrix}\tau(\mathcal{E}), \tag{5}$$

where α_t and α_l are constants and $\mathcal{E}$ is the electron energy. As a consequence of this equation K becomes $\alpha_t m_l/\alpha_l m_t$.[16] The results of calculations based on the assumption that $\alpha_t\tau(\mathcal{E})=\tau_0$, where τ_0 is a constant,[17] are given in Tables I to III for the various geometric conditions which were considered in the experimental measurements.

In general the elements of the conductivity tensor may be expressed in terms of integrals of the form

$$\mathfrak{I}_m=\int_0^\infty \frac{\tau^m\chi^{\frac{3}{2}}e^{-\chi}d\chi}{1+w^2\tau^2}, \tag{6}$$

where $m=1$, 2, or 3, w is related to the cyclotron frequency ω_c[7] but depends on the direction of **B** as well as its magnitude,[18] τ is the $\tau(\mathcal{E})$ of Eq. (5), and χ is the reduced energy $(\mathcal{E}/kT)$. These integrals can be expressed in closed form only for certain special relationships between τ and $\mathcal{E}$. When $w^2\tau^2\ll 1$ (which occurs when the magnetic field is very small), the denominator may be expanded in powers of $w^2\tau^2$ and Eq. (6) becomes

$$\mathfrak{I}_m=\langle\tau^m\rangle-w^2\langle\tau^{m+2}\rangle+w^4\langle\tau^{m+4}\rangle-\cdots, \tag{7}$$

where

$$\langle\tau^n\rangle\equiv\int_0^\infty \tau^n\chi^{\frac{3}{2}}e^{-\chi}d\chi. \tag{8}$$

This definition of $\langle\tau^n\rangle$ includes the $\frac{3}{2}$ power of energy

TABLE III. Galvanomagnetic coefficients for the magnetic field restricted to the $(1\bar{1}0)$-plane calculated using an energy-independent mean free time.

J	$M+1$ [a]	R [a]	PB^2/ρ_0 [a]
[110]	$\Delta(a_-a_3+2d^2)$	$yK\Delta R_\infty(a_3 f+2cd)/\gamma b$	$\Delta(df-ca_-)/\alpha\gamma$
[1$\bar{1}$0]	$\Delta(a_+a_3-2c^2)$	$yK\Delta R_\infty[2(cf+a_+d)\alpha+(a_3 f+2cd)\gamma]/b$	none

[a] In these expressions
$\Delta=(p-sb^2\alpha^2)[(p+sb^2\alpha^2)^2-4s^2b^4\alpha^2\gamma^2]/(a_+a_-a_3+2a_+d^2-2a_-c^2+4dcf+a_3f^2)$,
$a_+=(1+2yb^2\alpha^2)S_0+(z-y)S_2$, $a_-=S_0-(z-y)S_2$, $a_3=(1+yb^2\gamma^2)S_0$,
$c=(z-y)S_1+yb^2\alpha\gamma S_0$, $d=bz(\alpha S_0-\gamma S_1-\alpha S_2)+by(\gamma S_1+\alpha S_2)$,
$f=bz\gamma S_0-2b(z-y)\alpha S_1$, $S_0=p(p+sb^2\alpha^2)-2s^2b^4\alpha^2\gamma^2$, $S_1=sb^2\alpha\gamma(p-sb^2\alpha^2)$,
$S_2=sb^2\alpha^2(p+sb^2\alpha^2)-2s^2b^4\alpha^2\gamma^2$, $\alpha(=\beta)$ = direction cosine of **B** with respect to [100] or [010] axis and γ = direction cosine of **B** with respect to [001] axis.

[15] W. M. Bullis, Ph.D. thesis, Massachusetts Institute of Technology, June, 1956 (unpublished); Lincoln Laboratory Technical Report No. 115 (unpublished).

[16] It is often convenient to divide K into two parts: $K_m=m_l/m_t$ and $K_\tau=\alpha_l/\alpha_t$. Thus $K=K_m/K_\tau$.

[17] In general the parameter τ_0 will be a function of the temperature even in the range where it can be assumed to be independent of energy for purposes of integration over momentum space. However, since all the measurements which will be compared with these calculations were made at the same temperature (77°K), this dependence will be of no consequence.

[18] See reference 15, pp. 13–20.

inside the integral[10,19] so $\langle\tau^0\rangle=\Gamma(\frac{5}{2})$. In the limit of zero magnetic field, the conductivity approaches the value $\sigma_0=\eta\langle\tau\rangle$ where $\eta=4Ne^2\alpha_l(2K+1)/9\pi^{\frac{1}{2}}m_l$, N is the electron concentration, and e is the electronic charge. In the same limit, the Hall coefficient approaches the value $R_0=vKz\langle\tau^2\rangle/\eta\langle\tau\rangle^2$, where $v=e\alpha_l/m_lc$ and $z=(K+2)/(2K+1)$. The Hall mobility μ_H is defined as $R_0\sigma_0$, and the ratio of the Hall to conductivity mobility is given by $\mu_H/\mu=R_0/R_\infty$, where $R_\infty=(Nec)^{-1}$.

When **B** is restricted to the [100] or [110] direction, the low-field values of the galvanomagnetic coefficients are given by[20]

$$M_t\doteq\mu_H{}^2B^2[(\gamma/yzK)-1]\doteq M_{001}\doteq-P_{100}B^2/\rho_0 =M_{1\bar{1}0}-M_{110}, \quad (9)$$

$$M_l\doteq\mu_H{}^2B^2s^2yK\gamma/2z^2, \quad (10)$$

$$M_{45}=\tfrac{1}{2}(M_l+M_t)\doteq M_{100}=\tfrac{1}{2}(M_{110}+M_{1\bar{1}0}), \quad (11)$$

$$M_{110}\doteq\tfrac{1}{2}M_l, \quad (12)$$

$$M_{1\bar{1}0}\doteq\tfrac{1}{2}M_l+M_t, \quad (13)$$

$$P_{45}B^2/\rho_0=M_l-M_t, \quad (14)$$

where $\gamma=\langle\tau\rangle\langle\tau^3\rangle/\langle\tau^2\rangle^2$, $y=3/(2K+1)$ and $s=2(K-1)^2/3K$. The symbol $\doteq$ represents equalities which hold only at low magnetic fields (the low-field symmetry relations) while the remaining equalities hold for all values of the magnetic field. Measurements of the two coefficients M_t and M_l suffice, with the addition of R_0, to determine uniquely the low-field conductivity matrices[3,15] for the magnetic field in either a $\langle100\rangle$ or a $\langle110\rangle$ direction. Terms of higher order than those given in Eqs. (9) and (10) may be calculated but this turns out to be useful ouly in examining the low-field behavior of the Hall coefficient. The terms are so complicated that they will not be given explicitly. Instead, when necessary the Hall coefficient will be represented by the following relations[20]:

$$R^{001}=R_0(1+a_1B^2+a_2B^4+\cdots), \quad (15)$$

$$R^{110}=R_0(1+c_1B^2+c_2B^4+\cdots). \quad (16)$$

It is also necessary to consider the energy dependence of the scattering time. The simplest assumption is a straight power law:

$$\tau=l\mathcal{E}^\lambda, \quad (17)$$

for which:

$$\langle\tau^n\rangle=l^n(kT)^{n\lambda}\Gamma(\tfrac{5}{2}+n\lambda). \quad (17a)$$

The variation of λ with temperature[11] or resistivity allows in a very crude way for changes in the scattering mechanism as a function of either of these variables. A major difficulty is that when $n\lambda\geq-\frac{5}{2}$, the τ averages diverge.

Brooks[10,19] has pointed out that this divergence, which is of course not physical, can be removed if the integrals in the τ averages are cut off at a lower energy limit $\mathcal{E}_0$. Two expressions of this type will be considered here:

$$\tau=\tau_0, \quad 0\leq\mathcal{E}\leq\mathcal{E}_0; \qquad \tau=l\mathcal{E}^\lambda, \quad \mathcal{E}_0\leq\mathcal{E}\leq\infty, \quad (18)$$

for which

$$\langle\tau^n\rangle=l^n(kT)^{n\lambda}\left[\Gamma(\tfrac{5}{2}+n\lambda) +\sum_{\alpha=1}^{\infty}\frac{(-1)^{\alpha+1}n\lambda\chi_0{}^{\alpha+\frac{3}{2}+n\lambda}}{(\alpha-1)!(\alpha+\frac{3}{2})(\alpha+\frac{3}{2}+n\lambda)}\right], \quad (18a)$$

and

$$\tau=L\mathcal{E}^{\frac{3}{2}}, \quad 0\leq\mathcal{E}\leq\mathcal{E}_0; \quad \tau=l\mathcal{E}^\lambda, \quad \mathcal{E}_0\leq\mathcal{E}\leq\infty, \quad (19)$$

for which

$$\langle\tau^n\rangle=l^n(kT)^{n\lambda}\left[\Gamma(\tfrac{5}{2}+n\lambda) +\sum_{\alpha=1}^{\infty}\frac{(-1)^{\alpha+1}n(\lambda-\frac{3}{2})\chi_0{}^{\alpha+\frac{3}{2}+n\lambda}}{(\alpha-1)!(\alpha+\frac{3}{2}+n\lambda)(\alpha+\frac{3}{2}n+\frac{3}{2})}\right]. \quad (19a)$$

In order that the scattering function be continuous across $\mathcal{E}_0$, it is necessary that $\tau_0=l\mathcal{E}_0{}^\lambda$ and $L=l\mathcal{E}_0{}^{\lambda-\frac{3}{2}}$. Functions of the $\langle\tau^n\rangle$ which arise are tabulated elsewhere.[15] In either of these cases, the value of λ is fixed and the parameter χ_0 (or $\mathcal{E}_0$) is allowed to vary as a function of the resistivity or temperature. For values of $\chi_0<1$, the convergence of the series in (18a) and (19a) is quite good.

III. EXPERIMENTAL TECHNIQUES

The apparatus, sample preparation, and procedures have been described previously.[1] Most of the 77°K measurements were made on samples which were cut from the same crystal (No. 119) and had a net impurity concentration of about 1.6×10^{14} cm^{-3}. The doping material was antimony. For some measurements samples with higher and lower donor concentrations were used. In every case the carrier density was low enough that the samples were nondegenerate and high enough that intrinsic holes did not contribute significantly to the current.

The samples used for the 300°K measurements were similar to those used at 77°K. Except for the purest samples used, intrinsic holes did not contribute significantly to the current. The temperature was maintained constant by means of a water flow system. Water from a large well-stirred bath regulated by a mercury thermoregulator was circulated through a jacket surrounding the sample and its Teflon holder[1] by means of an automobile fuel pump. A cylindrical block of high-conductivity copper formed the base of the inner chamber and served to reduce transient changes in the temperature. The temperature was monitored by

[19] H. Brooks, *Advances in Electronics and Electron Physics*, edited by L. Marton (Academic Press, Inc., New York, 1955), Vol. 7, pp. 127–131.

[20] Definitions of the symbols in terms of the orientation of **B** and **J** are given in Table I.

a copper-Constantan thermocouple and remained constant to within ± 0.1C°.

The experimental determination of the Hall coefficient has been discussed.[1] In a similar manner the other coefficients are determined from potential measurements made for the four conditions obtained by reversing separately the current and magnetic field. The four voltages thus obtained are averaged so as to eliminate the even functions of **J** and the odd functions of **B**. Because of imperfect geometry (nonparallel faces or misalignment of the potential probes), local concentration gradients (which distort the lines of force), or slight misalignment of the sample in the magnetic field, there will be some intermingling of the magnetoresistance and planar Hall voltages. Since both of these coefficients are even functions of the magnetic field, this intermingling cannot be separated by the averaging process described above.

In the case of the magnetoresistance, the effect of the intermingling will usually be small and will be neglected. Unfortunately, it is by no means trivial and is probably the largest single source of error in the measurement of the magnetoresistance coefficient which may be expressed as[21]

$$M=(V_M/V_0)-1, \tag{20}$$

where V_M is the voltage per unit current measured along the direction of the current in the presence of a magnetic field and V_0 is the voltage per unit current measured between the same probes with no magnetic field. On the other hand, the potential drop between transverse probes in the absence of a magnetic field is ordinarily quite considerable. A correction to the planar Hall voltage is made to eliminate this potential which varies with the magnetic field due to the magnetoresistance effect. The corrected voltage V_P is then put in the formula[21]

$$P=2V_P t/IB^2 \sin 2\theta, \tag{21}$$

where t is the thickness of the sample in the direction perpendicular to both the current and planar Hall field, I is the magnitude of the current and θ is the angle between **I** and **B**. Because the necessary correction usually results in the taking of a small difference between two large numbers, the measurement of this coefficient is the least accurate of the three considered.

As in the previously reported work,[1] distortion effects due to shorting of the sample ends by the conducting solder were shown to be negligible by repeating some of the measurements after the sample had been cut in half along the long axis.

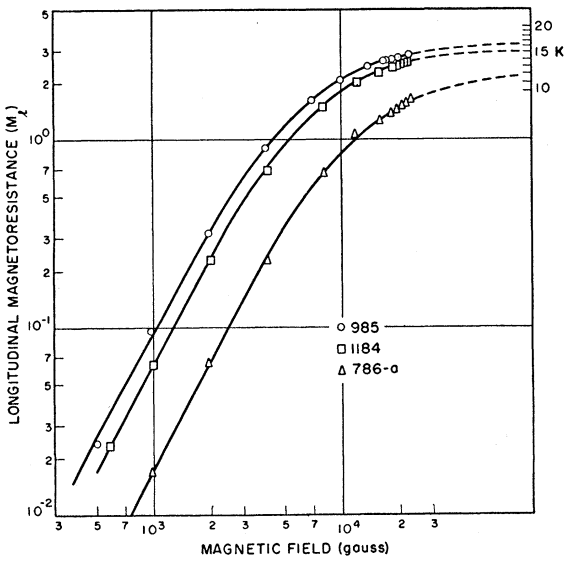

FIG. 1. Longitudinal magnetoresistance with **B** and **J** along the same cubic axis as a function of the magnetic field. Theoretical infinite-field limits for integral values of K are shown at the right edge of the figure. ($T=77$°K.)

IV. RESULTS AT 77°K

A. Field Dependence of the Coefficients

In general, the infinite-field limit of the longitudinal magnetoresistance is independent of the form of the energy dependence of τ as long as the form of the tensor is as assumed in Eq. (5). For germanium, the orientation in which this limit is most strongly dependent on K is the one where **B** and **J** are directed along the same cubic axis. In this case the value of the coefficient approaches $(2K+1)(K+2)/9K$. Measurements of the longitudinal magnetoresistance for this orientation in three samples of different impurity content are shown as a function of the magnetic field in Fig. 1.

Although the extrapolation is not very precise on the log-log plot, it is clear that the curves do not approach the same limit. Values of K appear to vary from about 16 for $N\approx 5.4\times 10^{13}$ cm^{-3} to about 12 or 13 for $N\approx 5.2\times 10^{14}$ cm^{-3}. Unfortunately the values of the coefficient at the highest available fields do not fall on the inverse-square portion of the theoretical curve and a linear extrapolation such as that done for the Hall coefficient[1] is not possible. Since a calculation by Herring[22] indicates that the effect of small variations in the impurity concentration is to cause the measured value of the high-field limit to be different than the value calculated for homogeneous material, only estimates of the value of K are possible.

Measurements of all the coefficients listed in Table I were made as a function of the magnetic field for samples cut from crystal 119. The two Hall coefficient curves have been previously presented[23] and are not

[21] In the experiment the current is maintained nearly constant but corrections must be made to allow for the slight variations present. It should be observed that $P=2G$, where G is the planar Hall coefficient of reference 8.

[22] C. Herring (private communication).

[23] Reference 1, Fig. 5. The theoretical curves shown were calculated for $K=19$ but the change to 15 does not appreciably affect the value of τ_0 ($\approx 2.4\times 10^{-12}$ sec, $b=5\times 10^{-4}B$) found there.

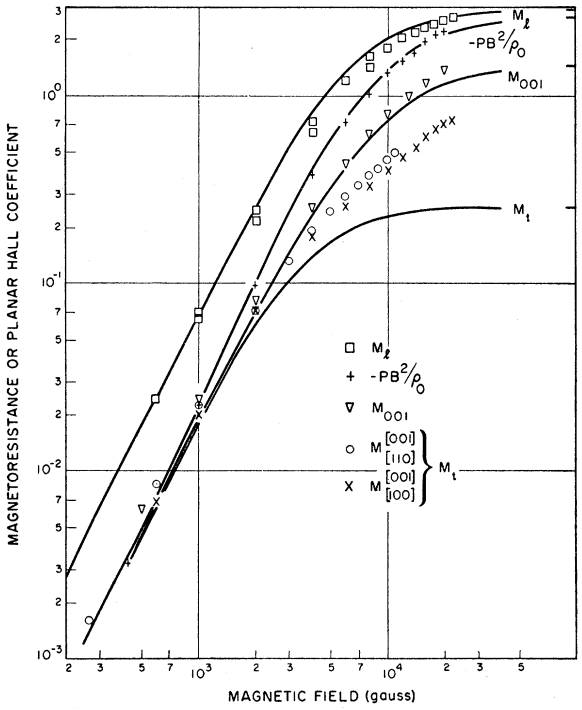

FIG. 2. Magnetoresistance[20] and planar Hall coefficient[20] as a function of the magnetic field for samples cut from crystal 119. The solid curves are calculated from the expressions of Table I with $K=15$ and $b=5\times10^{-4}B$. Theoretical infinite-field limits for $K=15$ are shown at the right edge of the figure. ($T=77$°K.)

repeated here. The magnetoresistance coefficients M_t, M_l, and M_{001} and the planar Hall coefficient P_{100} (normalized by the factor B^2/ρ_0) are shown as functions of the magnetic field in Fig. 2. The solid curves are calculated from the expressions given in Table I with $K=15$ and $b=5\times10^{-4}B$. The theoretical infinite-field limits are shown at the right edge of the figure. It can be seen that deviations from the theory at high fields increase as **J** and **B** become perpendicular. These deviations cannot be explained by assuming any reasonable power law for $\tau(\mathcal{E})$. The calculation by Herring[22] suggests that these deviations may be due to small variations in the impurity concentration.

Measured values of the magnetoresistance coefficients M_{100}, M_{110}, and $M_{1\bar{1}0}$ are shown as functions of the magnetic field in Fig. 3. In addition, values of M_{110} and $M_{1\bar{1}0}$ computed from the measured values of M_{100} and P_{100} are also shown. Again, the solid curves are calculated from the expressions in Table I for the same conditions as those in Fig. 2. The seven coefficients M_l, M_t, M_{100}, M_{001}, P_{100}, R^{001}, and R^{110} suffice to determine uniquely all the nonzero components of the resistivity tensor[3,15] when **B** is in either a ⟨100⟩ or a ⟨110⟩ direction.

All the coefficients for which the current is in a ⟨100⟩ direction were also determined as a function of the magnetic field for sample 985 which was slightly more pure than the group of samples from crystal 119. Similar results were obtained which could be fitted by using slightly higher values of K and τ_0. Again the anomalous behavior of the transverse magnetoresistance at high fields was observed.

TABLE IV. Values of the angles ϕ, ϕ', and ψ for cardinal directions of **B**.

B	[100]	[110]	[010]	[$\bar{1}$10]	[$\bar{1}$00]
ϕ[a]	0°	45°	90°	135°	180°
B	[110]	[010]	[$\bar{1}$10]	[$\bar{1}$00]	[$\bar{1}\bar{1}$0]
ϕ'[b]	0°	45°	90°	135°	180°
B	[110]	[111]	[001]	[$\bar{1}\bar{1}$1]	[$\bar{1}\bar{1}$0]
ψ[c]	0°	~35°	90°	~145°	180°

[a] **J**: [100] or [001].
[b] **J**: [110].
[c] **J**: [110] or [1$\bar{1}$0].

B. Angular Dependence of the Coefficients

Measurements of the three galvanomagnetic coefficients as a function of the angle between the current and magnetic field[24] were made in a magnetic field of 10 000 gauss for the orientations listed in Tables II and III. The magnetoresistance coefficients, Hall voltages[25] and planar Hall voltages[25] are shown in Figs. 4, 5, and 6, respectively. Values of the angles ϕ, ϕ', and ψ are given for cardinal directions of **B** in Table IV. The solid curves are calculated from the relations given in Tables II and III for $b=5$ and $K=15$. Equation (9) of Bullis

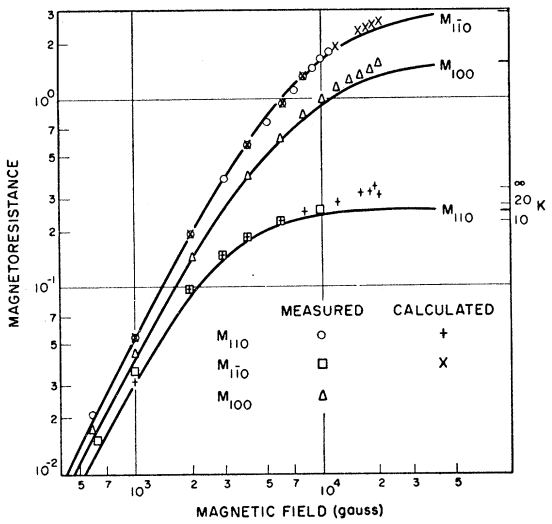

FIG. 3. Magnetoresistance[20] as a function of the magnetic field for samples cut from crystal 119. The solid curves are calculated from the expressions of Table I with $K=15$ and $b=5\times10^{-4}B$. Theoretical infinite-field limits for $K=15$ are shown at the right edge of the figure. In addition the theoretical infinite-field limit of M_{110} is shown for $K=10$, 20, and ∞. The calculated values of M_{110} and $M_{1\bar{1}0}$ were computed from measured values of M_{100} and P_{100}. ($T=77$°K.)

[24] In the cases where the current is always perpendicular to the magnetic field, the angle is defined arbitrarily as indicated in Table IV.

[25] Voltages rather than coefficients are given in these cases because of the uncertainty in the value of the measured angle. See reference 1.

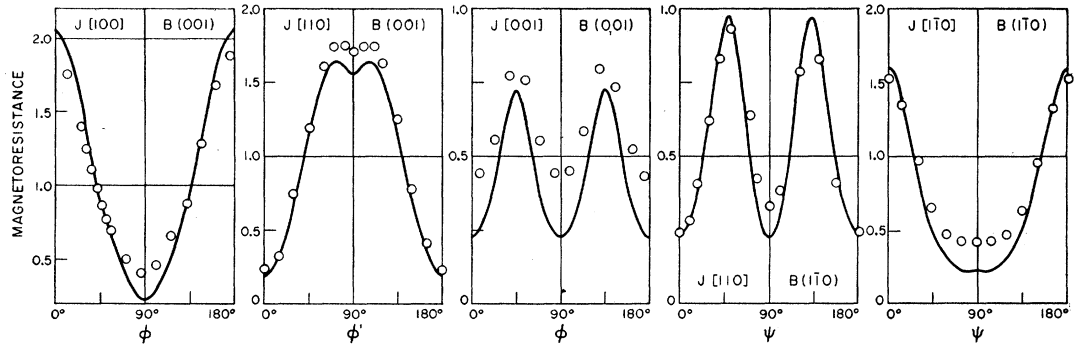

FIG. 4. Magnetoresistance as a function of the angle between current and magnetic field for samples cut from crystal 119. The solid curves are calculated from the expressions of Tables II and III with $K=15$ and $b=5$. Experimental data were taken at $T=77°$K and $B=10\,000$ gauss. ($\phi=\alpha$, $\phi'=\alpha-45°$, $\psi=90°-\gamma$.)

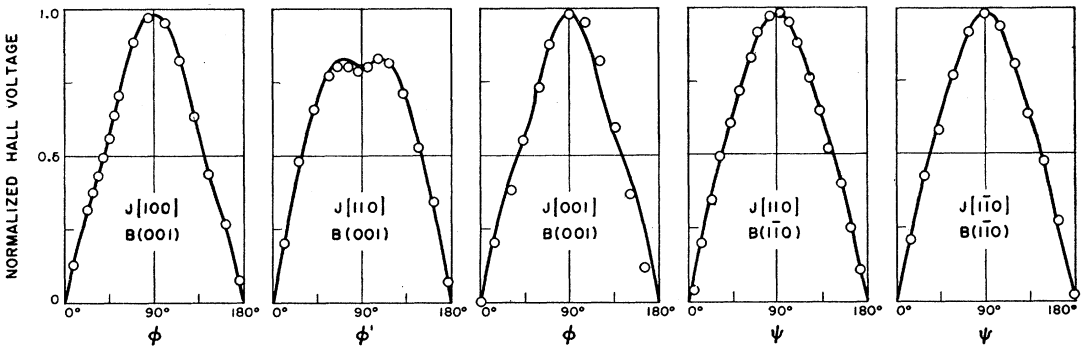

FIG. 5. Hall voltage ($R\sin\theta/R_\infty$) as a function of the angle between current and magnetic field for samples cut from crystal 119. The solid curves are calculated from the expressions of Tables II and III with $K=15$ and $b=5$. Experimental data were taken at $T=77°$K and B = 10 000 gauss. ($\phi=\alpha$, $\phi'=\alpha-45°$, $\psi=90°-\gamma$.)

and Krag[1] and Eq. (21) were used to determine the Hall and planar Hall voltages, respectively.

The principal features of the experimental data are duplicated by the calculated curves. It is not surprising that the quantitative agreement between theory and experiment is not better because of the drastic simplifying assumptions made in assuming an energy-independent mean free time. Measurements of most of these coefficients were also made at 2000 gauss[15] and compared with calculations made assuming $b=1$. Similar semiquantitative agreement was obtained but the results are not as striking at the lower fields where departures from the quadratic expressions are not pronounced.

V. RESULTS AT 300°K

A. Magnetoresistance Measurements

The results of the low-field magnetoresistance measurements are summarized in Table V which also gives the zero-field coefficients ρ_0, R_0, and μ_H. In addition to the six samples measured in this series, the data reported by Pearson and Suhl[9] for an 11.5 ohm-cm sample are also listed. The values given in Table V were derived from curves of M/B^2 extrapolated to zero field. A typical plot is shown in Fig. 7. Also shown in this plot is $-P_{100}/\rho_0$ which can be seen to depart from the values of M_t/B^2 and M_{001}/B^2 at the higher fields. At still higher fields M_t and M_{001} will separate.[26] The departure of M_{100} from M_{45} (the mean between M_l and M_t) can also be observed in Fig. 7. The data are plotted as a function of the zero-field resistivity in Fig. 8. It will be noted that there is an upswing at the high-resistivity end of the curve. This is consistent with the

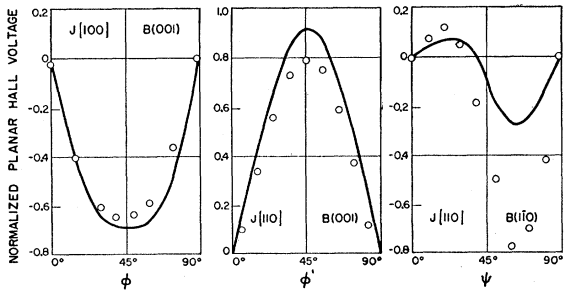

FIG. 6. Planar Hall voltage ($PB^2\sin2\theta/2\rho_0$) as a function of the angle between current and magnetic field for samples cut from crystal 119. The solid curves are calculated from the expressions of Tables II and III with $K=15$ and $b=5$. Experimental data were taken at $T=77°$K and $B=10\,000$ gauss. ($\phi=\alpha$, $\phi'=\alpha-45°$, $\psi=90°-\gamma$.)

[26] See Fig. 2.

TABLE V. Summary of low-field magnetoresistance data—300°K. M_l, M_{100}, and M_t were derived from curves of M/B^2 extrapolated to zero field. M_{110}, $M_{1\bar{1}0}$ and M_{45} were computed from M_l and M_t using Eqs. (11) to (13).

Sample No.	1184	1498	1262	786a	1261	1260	$P-S$ factor
ρ_0 (ohm-cm)	8.89	5.6[a]	3.2[a]	0.592	0.293	0.016	11.5
R_0 (cm³/coul)	33.4	20[a]	12[a]	1.80	0.90	0.023	44.0×10^{3}
μ_H (cm²/v-sec)	3.76	3.5[a]	3.7[a]	3.04	3.07	1.43	3.82×10^{3}
M_l/B^2 (gauss^{-2})	17.2	16.7	16.3	12.2	10.4	1.95	19.2×10^{-10}
M_{100}/B^2 (gauss^{-2})	12.7	11.8	11.7	8.5	7.1		$\times10^{-10}$
M_t/B^2 (gauss^{-2})	8.2	7.5	7.2	5.0	3.9	0.66	9.0×10^{-10}
M_{110}/B^2 (gauss^{-2})	8.6	8.4	8.2	6.1	5.2	0.98	9.6×10^{-10}
$M_{1\bar{1}0}/B^2$ (gauss^{-2})	16.8	15.9	15.4	11.1	9.2	1.64	18.6×10^{-10}
M_{45}/B^2 (gauss^{-2})	12.7	12.1	11.8	8.6	7.2	1.30	14.1×10^{-10}

[a] Samples 1498 and 1262 were very nonuniform and these values are very crude averages.

observations of Goldberg and Davis[11] who attributed a similar upswing above 270°K (in an 11.5 ohm-cm sample) to the influence of intrinsic holes. At 300°K approximately 3% of the carriers in sample 1184 are holes and in the 11.5 ohm-cm samples the hole density is somewhat higher.[27]

K may be computed directly[28] from the measured values of M_l and M_t provided that the Hall mobility μ_H is known. In Fig. 9, μ_H is plotted as a function of ρ_0. Values due to Pearson and Suhl[9]; Mason, Hewitt, and Wick,[14] and Debye and Conwell[29] are also shown. Because of the wide scatter[15] in the experimental points, a central curve and two other curves at $\pm6\%$ of the central value are drawn through the experimental points. The values of K computed from M_l, M_t, and the central value of μ_H are plotted in Fig. 10. K is about 17.3 for resistivities higher than 0.1 ohm-cm but falls off at lower resistivities. Similar qualitative behavior is observed for the other values of μ_H. The strong dependence of K on the Hall mobility is demonstrated by the lower curve in Fig. 10 which was computed using the $+6\%$ value of μ_H.

In order to interpret the data as a function of ρ_0, it is necessary to assume that τ varies with the energy in some specified way. If the simple power law, Eq. (17), is assumed, the variation of λ with ρ_0 is as shown[30] in Fig. 11. The analysis is similar to that used in interpreting data taken as a function of temperature.[11] If Eq. (18) or (19) is assumed and λ is taken as -0.66 to agree with the temperature dependence of the mobility found by Prince,[31] the resulting values of χ_0 are as shown[30] in Fig. 12.

From the value of λ or χ_0 determined in this way, it is possible to determine other relationships involving the collision time. The simplest of these is the ratio of

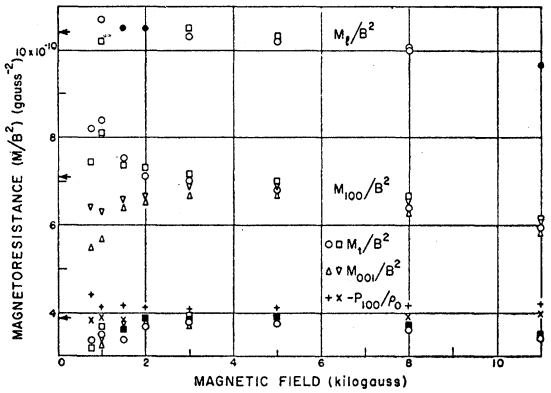

FIG. 7. Magnetoresistance[20] of sample 1261 at 300°K as a function of magnetic field. The arrows indicate the value of the coefficients extrapolated to zero field.

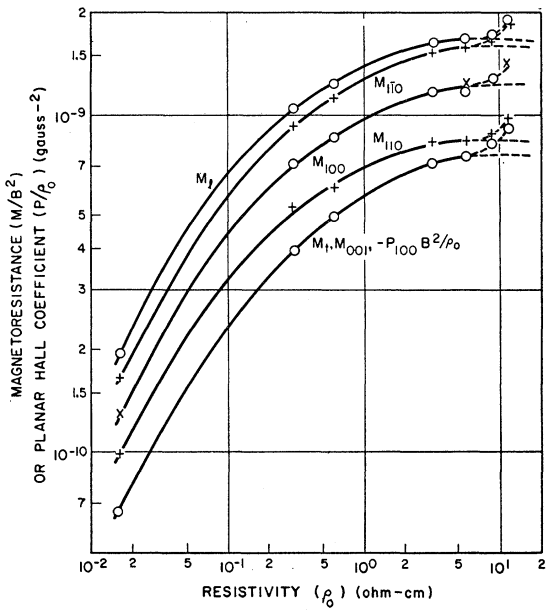

FIG. 8. Low-field magnetoresistance[20] at 300°K as a function of the zero-field sample resistivity.

[27] Apparently the presence of a reasonably small percentage of holes does not affect the symmetry properties. This is indicated by the angular measurements (at 4000 gauss) by Pearson and Suhl[9] and by angular measurements (at 6000 gauss) taken on sample 1184 which yielded similar results.

[28] Reference 15, Eq. (2-43); Reference 11, Eq. (11).

[29] P. P. Debye and E. M. Conwell, Phys. Rev. **93**, 693 (1954).

[30] Because of the uncertainty in the precise values for K, the values of λ (Fig. 11), χ_0 (Fig. 12), μ_H/μ (Fig. 13), c_1 and c_2 (Fig. 16), and a_1 and a_2 (Fig. 17) are intended only to indicate the trend with resistivity.

[31] M. B. Prince, Phys. Rev. **92**, 681 (1953).

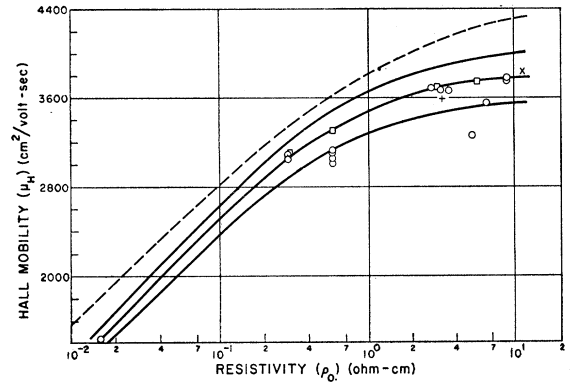

FIG. 9. Hall mobility at 300°K as a function of the zero-field sample resistivity. The dashed curve is taken from the data of Debye and Conwell.[29] The upper and lower solid curves are drawn at ±6% of the central curve through the experimental points. Points due to Mason, Hewitt, and Wick[14] (+) and Pearson and Suhl[9] (×) are also shown.

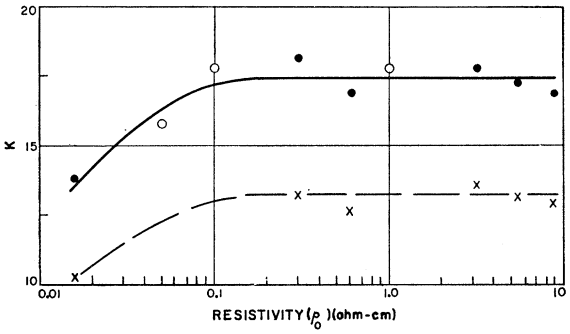

FIG. 10. Anisotropy factor K as a function of the zero-field sample resistivity. The solid circles were computed using the central value of μ_H. Open circles were computed using data derived from the curves of Figs. 8 and 9 at points which were not measured explicitly. The crosses were derived from the +6% value of μ_H.

Hall to conductivity mobility, which is shown[30] in Fig. 13 for the three scattering relations. It can be seen that all the values are somewhat less than the value of about 1 reported by Morin[32] for very pure samples. The points based on Eqs. (18) and (19) fall nearly within the experimental error of Morin's measurements at the high-resistivity end of the curve but those based on Eq. (17) are appreciably lower.

B. Hall Measurements

Curves of R^{001} and R^{110} normalized to their value at zero magnetic field are plotted as a function of the field in Figs. 14 and 15, respectively. The dashed curves are the empirical relationships reported by Mason, Hewitt, and Wick[14] for 3.18 ohm-cm cylindrical samples. The theoretical curve in Fig. 14 was calculated from the first of Eqs. (4.14) of Abeles and Meiboom[2] using parameters ($K=17.4$, $\mu_H=3770$ cm²/volt-sec) corresponding to samples 805a and 1184. Since this calculation is based

[32] F. J. Morin, Phys. Rev. **93**, 62 (1954).

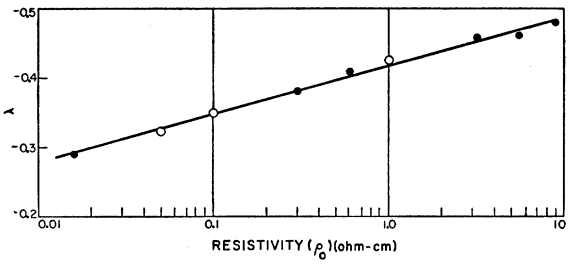

FIG. 11. The exponent λ of Eq. (17) as a function of the zero-field sample resistivity. The solid points were computed using measured magnetoresistance data while the open points were derived from the curves of Fig. 8 at resistivities which were not actually measured. The value[30] of K was taken from the solid curve of Fig. 10.

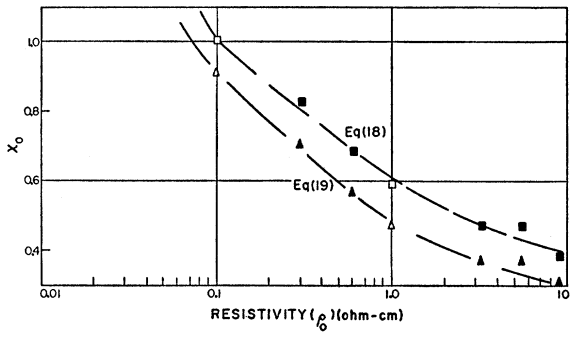

FIG. 12. The reduced transition energy χ_0 as a function of the zero-field sample resistivity. The solid points were computed using measured magnetoresistance data while the open points were derived from the curves of Fig. 8 at resistivities which were not actually measured. The value[30] of K was taken from the solid curve of Fig. 10.

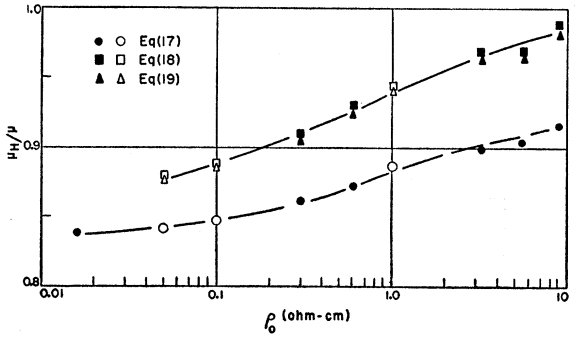

FIG. 13. The mobility ratio as a function of the zero-field sample resistivity calculated from Eqs. (17), (18), and (19) using the parameters of Figs. 11 and 12 and the value[30] of K taken from the solid curve of Fig. 10.

on the constant mean-free-path approximation [$\lambda=-\frac{1}{2}$ in Eq. (17)], it is clear that this assumption is not adequate to explain the field dependence of the Hall coefficient at 300°K.

The coefficient R^{110} (Fig. 15) departs from its zero-field value at higher and higher fields as the resistivity decreases. This is consistent with the fact that as ρ_0 (or τ) decreases, the fields for which $w^2\tau^2 \ll 1$ become larger. For the coefficient R^{001} (Fig. 14) this is no longer

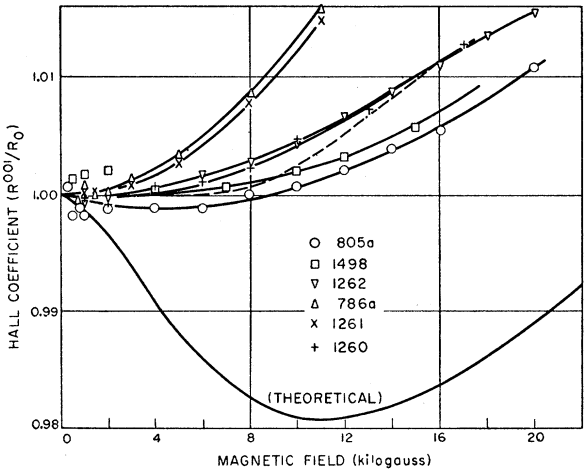

FIG. 14. Normalized Hall coefficient R^{001}/R_0 at 300°K as a function of the magnetic field. The theoretical curve is calculated from the relation given by Abeles and Meiboom[2] for $K=17.4$, $\mu_H=3770$ cm²/volt-sec and should correspond to sample 805a. The dashed curve is an empirical result of Mason, Hewitt, and Wick[14] for a 3.18 ohm-cm sample ($a_1=0$, $a_2=+2.4\times10^{-19}$).

true. Here the coefficients appear to depart from the zero-field value at lower fields as the resistivity decreases down to about 0.5 ohm-cm where the trend reverses and the behavior becomes normal. This implies that for the higher resistivities, a term is operating to hold R close to R_0 even though $w^2\tau^2$ is not small compared to 1.

These observations agree qualitatively with calculations of the coefficients of Eqs. (15) and (16) made using the scattering laws of Eqs. (17) to (19) and the parameters derived from the magnetoresistance data of Sec. V-A. If Eq. (17) is used, the second (a_2 and c_2) and subsequent coefficients diverge and only the leading term can be calculated. It is found that a_1 is negative for large resistivities and becomes positive for low resistivities. The sign change occurs at $\lambda\approx-0.36$. On the other hand, c_1 is always positive and decreases with

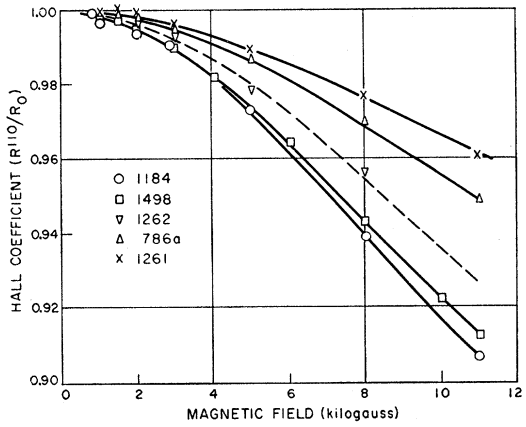

FIG. 15. Normalized Hall coefficient R^{110}/R_0 at 300°K as a function of the magnetic field. The dashed curve is an empirical result of Mason, Hewitt and Wick[14] for a 3.18 ohm-cm sample ($c_1=-7.9\times10^{-10}$, $c_2=+1.55\times10^{-18}$).

decreasing resistivity. This monotonic decrease is noted in both c_1 and c_2 when Eqs. (18) and (19) are used. Values are shown[30] in Fig. 16 together with experimental values derived from plots of R^{110} *vs* B^2. It can be seen that the two sets of points follow the same trend although the numerical agreement is not exact. Values of a_1 and a_2 are shown[30] in Fig. 17. The change of sign can be noted in both coefficients. In addition it can be seen that both coefficients decrease in magnitude at very low resistivities where the ratio $w^2\tau^2:1$ again becomes dominant. Although the data are not precise enough to enable experimental values of a_1 and a_2 to be determined, the calculated values reproduce the qualitative features of the curves. The numerical values are too high for quantitative agreement.[33]

It is possible to compute values of χ_0, K, and μ_H from the experimental values of c_1 and c_2. When this is done,

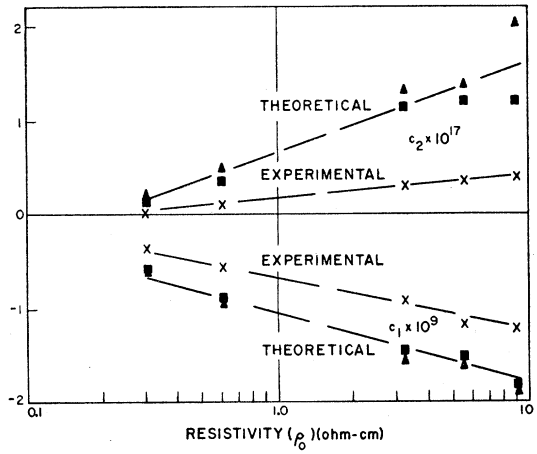

FIG. 16. Hall parameters of Eq. (16) as a function of the zero-field sample resistivity. The points were computed by using the magnetoresistance data of Figs. 11 and 12 and the scattering laws of Eqs. (18) and (19). The value[30] of K was taken from the solid curve of Fig. 10. The experimental points were derived from plots of R^{110} *vs* B^2.

low values of K (10 to 12) and very high values of χ_0 and μ_H are required for self consistency. These results which are obtained with either Eq. (18) or (19) are not compatible with the other experimental data and serve to indicate the inadequacy of the assumptions made concerning the scattering functions.

VI. CONCLUSIONS

The anisotropy factor K has been evaluated from low-field magnetoresistance measurements at 300°K and from high-field longitudinal magnetoresistance measurements at 77°K. A value of 17.3 is found at 300°K for samples with resistivities greater than about 0.1 ohm-cm. This is in good agreement with the value

[33] Although thermomagnetic potentials (e.g., Ettinghausen) could cause experimental errors in the Hall data, it is strongly felt that any such errors are negligible compared to those resulting from the approximation for $\tau(\mathcal{E})$.

of 17.2 found from pulsed high-field longitudinal magnetoresistance measurements,[34] but it is somewhat higher than the low-field values reported by others.[10–12,35] The wide variations in the reported values of K determined from low-field measurements may be attributed to the strong dependence of K on the Hall mobility μ_H which is difficult to measure precisely. At 77°K the value of K was found to decrease from about 16 to about 12 or 13 as the impurity concentration was increased from 5.4×10^{13} to 5.2×10^{14} cm^{-3}.

When determined from galvanomagnetic data, K is a measure of the anisotropy of the mobility (τ/m). The

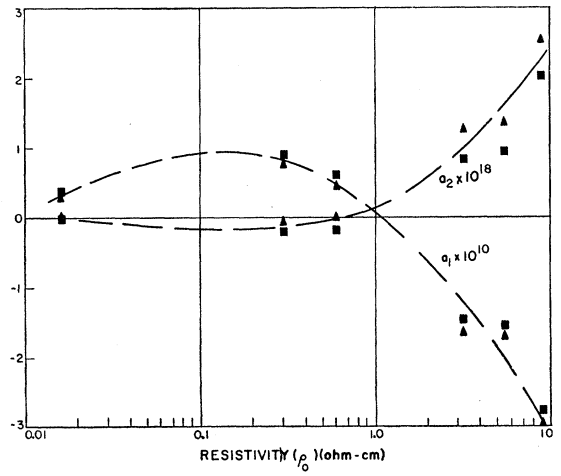

FIG. 17. Hall parameters of Eq. (15) as a function of the zero-field sample resistivity. The points were computed by using the magnetoresistance data of Figs. 11 and 12 and the scattering laws of Eqs. (18) and (19). The value[30] of K was taken from the solid curve of Fig. 10.

mass anisotropy K_m has been found[7] to be about 20 at 4°K. It is reasonable to assume that this value changes only slightly, if at all, with temperature. It is therefore possible to calculate the scattering anisotropy K_τ with the result that $K_\tau \approx 1.2$ at 300°K for lattice scattering (including intervalley scattering,[5] if present). As the temperature is reduced (with constant impurity density) or as the resistivity is reduced (at constant T), the relative effect of impurity scattering increases and K_τ becomes larger as predicted by Ham.[36]

These experiments further confirm the usefulness of galvanomagnetic measurements in studying the symmetry properties of the band structure of materials by utilizing either the energy-independent mean-free-time formalism[1] or the low-field symmetry relations.[37] In addition a small amount of information relative to the energy dependence of τ at 300°K may be deduced from the low-field magnetoresistance data. The parameters in the assumed scattering functions behave in the expected way as the resistivity decreases and the relative importance of impurity scattering increases. The usefulness of the transition energy concept[19] is demonstrated by the agreement with measured values of the mobility ratio. The quantitative inadequacy of the theory which arises in connection with the low-field behavior of the Hall coefficient is probably due to the inadequacy of the drastic approximations made for $\tau(\mathcal{E})$ coupled with the fact that the low-field expansion may no longer be valid after the initial terms when these approximations are used.[9]

VII. ACKNOWLEDGMENTS

The author would like to acknowledge the assistance and support of the many members of the Solid State Group of Lincoln Laboratory whose contributions were instrumental in the completion of this work, particularly Mr. W. E. Krag and Dr. L. Gold whose contributions were especially helpful. Mr. A. M. Sanderson assisted in the mechanical details of the construction of the apparatus and Miss M. C. Glennon assisted with many of the calculations. Special thanks is due Professor W. P. Allis for his constant encouragement and many hours of helpful discussions.

[34] H. P. Furth and R. W. Waniek, Phys. Rev. **104**, 343 (1956).
[35] M. Glicksman, Phys. Rev. **102**, 1496 (1956).
[36] F. S. Ham, Phys. Rev. **100**, 1251(A) (1955).
[37] G. L. Pearson and C. Herring, Physica **20**, 975 (1954).